FRONT TRACKING FOR ONE-DIMENSIONAL QUASILINEAR HYPERBOLIC EQUATIONS WITH VARIABLE COEFFICIENTS

KNUT–ANDREAS LIE

ABSTRACT. A new front tracking method is developed for the variable coefficient equation $u_t + V(x,t)f(u)_x = 0$. The method is a generalization of Dafermos' method for the constant coefficient case and is well-defined also for certain discontinuous velocity fields V. We give an explicit inequality stating the stability with respect to flux function, velocity field, and initial data. The numerical method is unconditionally stable and has linear convergence. It is well suited for numerical calculations, as is demonstrated in four examples.

1. INTRODUCTION

We consider the quasilinear, variable coefficient equation

$$u_t + V(x,t)f(u)_x = 0, \qquad u(x,0) = u_0(x). \tag{1}$$

The equation describes the convection of a scalar quantity u in a forcing velocity field $V(x,t)$. A motivation for this study is that (1) occurs as an essential step in various operator splittings: dimensional splitting [26] for the multidimensional analogue of (1); two-phase flow with capillary forces [16, 19]; two-phase, multicomponent flow [11]; and convection–diffusion equations [7, 18]. Moreover, the ideas described here easily carry over to other equations, for instance $u_t + V(x,t)u_x + f(u)_x = 0$ which occurs in models for glaciers [18] and sedimentation [5].

The focus will be on the following two questions: How is a numerical approximation to a possibly discontinuous solution of (1) computed efficiently? Moreover, how does the solution depend on flux function, velocity field, and initial data?

To make numerical approximations to (1), we will introduce a front tracking method. The method is a modification of a method that was suggested by Dafermos [6] in the 70s to study initial value problems for the nonlinear hyperbolic equation $u_t + f(u)_x = 0$. A related method had been used a decade earlier by Barker [1] for numerical studies at Sandia National Laboratories. Dafermos observed that if the flux function f is convex and piecewise linear, the solution of the Riemann problem is a step function (piecewise constants). If the initial data u_0 is within the class of step functions, an analytical solution of the Cauchy problem can be constructed by superposition of simple Riemann problems. The solution will remain piecewise constant for all time, and thus within the same class of functions, since all wave interactions lead to new Riemann problems. By solving these Riemann problems each time two or more waves interact, a global solution can be established. In the general case, approximating the flux function by a sequence of piecewise linear functions and the initial data by a sequence of

Date: April 14, 2000.

1991 *Mathematics Subject Classification.* 35L60, 65M12, 65M15, 65M99.

Key words and phrases. Variable coefficients, scalar conservation laws, front tracking, error analysis, numerical methods.

My research has been supported in part by the Research Council of Norway under grant 100555/410.

step functions gives a compact sequence of approximate solutions converging to the solution of the Cauchy problem.

Numerical studies based upon Dafermos' method were reported by Hedstrom [12, 13] for scalar problems and the p-system. Moreover, Swartz and Wendroff [33] reported on a hybrid method with moving grid points, which was based on Dafermos' construction. Zheng [35] showed that Dafermos' construction was well-posed by proving that an arbitrary point $t \in [0, \infty)$ can be reached in a finite number of steps.

Unaware of these early papers, Holden, Holden and Høegh–Krohn [15, 14] rediscovered the method and proved that the construction was well-defined also for non-convex flux functions. They named the method *front tracking*—front referring to the discontinuities and tracking to the process of computing collisions and resolving interactions. Front tracking is a very robust numerical method for scalar, one-dimensional conservation laws. In fact, the method works for any (Lipschitz continuous) flux function, as opposed to some Riemann based, high-resolution methods that have problems at inflection points. The method is very fast, unconditionally stable, and first order even with discontinuous solutions [27]. A second-order alternative was presented by Lucier [27].

Motivated by applications to reservoir simulation, Gimse and Risebro [8, 9, 10] presented an extension of the one-dimensional front tracking method to conservation laws with discontinuous flux functions (see also [20]). Holden [17] used front tracking to study the Buckley–Leverett equation with a spatially stochastic flux occurring in the simulation of secondary oil recovery.

For systems, the front tracking algorithm needs a reformulation, as the idea of making piecewise linear approximations will not work for most equations. This was done by Risebro [30], who presented the new method as an alternative to Chorin's random choice method. Starting with the Lax construction and using the local coordinate systems of wave curves around two constant states one can construct piecewise constant approximations to Riemann solutions by keeping shocks and contact discontinuities and replacing rarefaction waves by step functions taking values sampled along the continuous wave curve. For applications of front tracking to specific systems, see [31, 32, 23].

A closely related method is the *wave front tracking* method of Bressan, which has been used to show stability, and thereby uniqueness, of solutions of systems in one spatial dimension [3, 4]. Moreover, the method is related to the large time step method of LeVeque [24, 25], which is simpler in the sense that it does not resolve nonlinear wave interactions.

In the current paper, we show how the front tracking ideas carry over to the scalar, variable coefficient equation (1). The Riemann problem for this equation has the same permissible discontinuities (for positive a velocity field V) as $u_t + f(u)_x = 0$, but instead of following straight lines, the discontinuities travel along paths satisfying an ordinary differential equation. By carefully choosing an approximation to the velocity field, one is able to compute these paths explicitly. The form of the shock paths is not essential to Dafermos' method, and it can therefore be extended to the variable coefficient case. We show that the new method is well-defined under some mild restrictions on the velocity field V, and that it can be used to obtain a sequence of approximations converging to the weak entropy solution of the Cauchy problem (1) in the sense of Kružkov [21]. For $V = V(x)$ an obvious alternative would be to transform (1) using $\frac{\partial}{\partial y} = V \frac{\partial}{\partial x}$. Although this approach would work well if V has constant sign, we believe that it gets rather cumbersome when V changes sign in the domain. Moreover, how to define a similar approach for time dependent velocity fields is a difficult task, if possible, and we will therefore not pursuit it further here.

Existence and uniqueness of discontinuous solutions were proved by Kružkov[21] under certain requirements for a more general equation. He proposed an *entropy condition* to identify the unique physical solution. Using this condition, we turn to investigate how solutions are sensitive to changes in flux function, velocity field, and initial data. Our analysis is inspired by, and extends, a theorem proved by Lucier [27] for the constant coefficient case. The dependence result can then be applied to prove stability and linear convergence of the new front tracking scheme.

The outline of the paper is as follows. In Section 2 a sequence of approximate weak solutions is constructed. We show that the limit is the unique entropy solution in the Kružkov sense, thus giving a partial answer to our first question. In Section 3, the second question is fully answered in the form of an explicit inequality stating the stability of solutions with respect to f, V, and u_0. The first question is answered in Section 4, which contains a more thorough discussion of the front tracking construction used as a numerical method. Using the stability result from Section 3 we verify that the method has linear convergence. In Section 5, four numerical experiments are presented.

2. Construction of a Weak Solution

In this section we describe the front tracking construction in more detail. Assume that the velocity field $V(x,t)$ is differentiable with respect to x. Then equation (1) can be transformed—without changing the generalized solutions—by adding and subtracting a term $V_x(x,t)f(u)$ to yield an equation on conservative form (see (8) below),

$$u_t + \frac{\partial}{\partial x}\big(V(x,t)f(u)\big) - V_x(x,t)f(u) = 0.$$

Recall that for differentiable velocity fields a weak solution of (1) is defined to satisfy

$$\int_{\mathbf{R}}\int_0^\infty \big\{u\phi_t + f(u)\big(V(x,t)\phi\big)_x\big\}\,dtdx + \int_{\mathbf{R}} u(x,0)\phi(x,0)\,dx = 0 \tag{2}$$

for an arbitrary test function ϕ. If $V(x,\cdot)$ is merely Lipschitz continuous, the weak solution can be defined similarly. This follows from a standard argument in which we replace V by a smooth approximation $V^\varepsilon = \omega_\varepsilon * V$ and then subsequently let ε tend to zero. Here ω_ε is a standard mollifier function. In this case, $(V(x,t)\phi)_x$ denotes the generalized derivative. With piecewise constant initial data, the initial value problem (1) is decomposed into a series of simple Riemann problems

$$u_0(x) = \begin{cases} u^-, & \text{when } x < 0 \\ u^+, & \text{when } x > 0. \end{cases}$$

Generally, Riemann problems admit both smooth waves (rarefactions) and discontinuities (shocks), but if the flux function is piecewise linear, the solution consists only of constant states separated by lines of discontinuity.

Weak solutions are not necessarily unique. To get a unique solution, an entropy condition must be introduced. Here we use a simplified version of a condition proposed by Oleinik [29]. Let u be between u^+ and u^-. Then the jump from u^- to u^+ is permissible provided

$$\operatorname{sgn} V(x,t)\cdot\frac{f(u)-f(u^+)}{u-u^+} \le s\cdot\operatorname{sgn} V(x,t) \le \operatorname{sgn} V(x,t)\cdot\frac{f(u)-f(u^-)}{u-u^-}, \tag{3}$$

for u between u^- and u^+. The associated shock speed s is given by

$$s = (f(u^+) - f(u^-))/(u^+ - u^-).$$

The entropy condition leads to a local convexification of the flux function, when solving the Riemann problem. Suppose that $V(x,t) > 0$ and $u^- < u^+$ and let f_c denote the lower convex envelope of f relative to the interval $[u^-, u^+]$. (The case $u^- > u^+$ is treated symmetrically, with f_c denoting the upper concave envelope). Since f is piecewise linear, then so is f_c. Let $\{u_i\}_{i=1}^N$ denote the breakpoints of f_c, such that $u_1 = u^-$ and $u_N = u^+$. Then the solution of the Riemann problem is

$$u(x,t) = \begin{cases} u_1, & \text{for } x < x_1(t) \\ u_i, & \text{for } x_{i-1}(t) \le x \le x_i(t), \quad i = 2, \dots, N-1, \\ u_N, & \text{for } x > x_{N-1}(t), \end{cases}$$

where each $x_i(t)$ satisfies a Rankine–Hugoniot condition

$$\frac{dx_i}{dt} = V(x_i,t)\Big(\frac{f_c(u_{i+1}) - f_c(u_i)}{u_{i+1} - u_i}\Big) = V(x_i,t)s_i. \tag{4}$$

If V is positive on an interval, the entropy condition on that interval is the same as for $u_t + f(u)_x = 0$. Thus, the permissible shocks are similar to those for the constant coefficient case, but the shock curves are not necessarily straight lines. However, as we shall see next, they are possible to compute explicitly in certain cases. Where the velocity field is negative, we can replace f by $-f$ and V by $-V$, or in other words, change the role of the upper and the lower convex envelope when determining f_c.

There exists a unique shock path satisfying the ordinary differential equation (4). If the function $V(x,t)$ has a simple form, the shock paths can be computed explicitly. For instance, if $V(x) = ax + b$ for nonzero a, the path of a shock with speed s starting from x_0 at time t_0 is given by

$$x(t) = \big(x_0 + \frac{b}{a}\big) \exp\big[as(t - t_0)\big] - \frac{b}{a}. \tag{5}$$

Similarly, if $V(t) = ct + d$, the path is given by

$$x(t) = s\big(\tfrac{1}{2}ct^2 + dt\big) - s\big(\tfrac{1}{2}ct_0^2 + dt_0\big). \tag{6}$$

These simple analytical expressions for the shock paths will be crucial when we derive the numerical method in Section 4. Then we will approximate an arbitrary velocity field by another velocity field that is either piecewise linear in x and piecewise constant in t, or piecewise constant in x and piecewise linear in t. For the general construction, however, it is sufficient that there is a unique path for each shock (4).

If the forcing velocity field has constant sign, the construction of a weak solution from Holden *et al.* [15] can now be repeated, only modifying the shock paths according to (4). First, connect all local Riemann solutions to give a global solution in x, consisting of constant steps separated by space-time rays. The solution is valid up to the first time when two waves from neighbouring Riemann problems interact. This interaction defines a new Riemann problem with left and right states given by the values immediately to the left and to the right of the collision point. The Riemann problem is solved as outlined above, thereby giving the global solution until the next interaction occurs, and so on.

When V changes sign, special care has to be taken as the entropy condition depends on the sign of V. Assume first that $V = V(x)$. In this case, zeros in the velocity are resolved automatically by the above construction since waves cannot cross a point or a region of zero velocity field due to (4). Moreover, we observe that there is nothing in the construction that prevents $V(x)$ from having discontinuities, as long as the sign is preserved across each jump, that is, $\operatorname{sgn} V(x^-) = \operatorname{sgn} V(x^+)$ at every point of discontinuity. Thus, the requirement that V is differentiable with respect to x can be relaxed.

Assume now that $V = V(t)$. At points $t = \tau$ where the velocity field changes sign we simply 'restart' the algorithm with initial data $u(x, \tau^-)$ and use $\operatorname{sgn} V(\tau^+)$ in the entropy condition to determine which envelope to choose for each initial Riemann problem. Finally, if the velocity field is zero in an interval, i.e., $V(t) = 0$ for $t \in [t_1, t_2]$, then the solution remains constant in this interval, $u(x,t) = u(x, t_1^-)$.

When constructing an approximate solution for an arbitrary $V = V(x,t)$ that contains both positive and negative values, we utilize the two special cases discussed above. That is, we define a mesh in (x,t) and consider an approximation $\widetilde{V}$ of V such that $\widetilde{V}(\cdot, t)$ has constant sign on each mesh cell. Moreover, we require that $\operatorname{sgn} \widetilde{V}(x^-, \cdot) = \operatorname{sgn} \widetilde{V}(x^+, \cdot)$ at every point of discontinuity in x. The purpose of the mesh is to 'discretize' the restarts that are needed in the algorithm when $V(\cdot, t)$ changes sign. (To see the problem, consider e.g., the velocity field $V(x,t) = t - x$).

Summing up, we have the following result:

Lemma 2.1. *Suppose that f is continuous and piecewise linear and that u_0 is a bounded step function of bounded variation. Furthermore, suppose that V is bounded and satisfies the two properties:*

(i) $\operatorname{sgn} V(x^-, t) = \operatorname{sgn} V(x^+, t)$ *at every point of discontinuity in x,*
(ii) *for each finite $0 < T$ there is a finite number of points $\tau < T$ such that* $\operatorname{sgn} V(x, \tau^-) \neq \operatorname{sgn} V(x, \tau^+)$ *for some x.*

Then the solution of equation $u_t + V(x,t) f(u)_x = 0$ can be computed by the front tracking algorithm. The solution $u(x,t)$ is a step function for fixed times t, and $u(x,t) \in \{u_0\} \cup \{u | f' \text{ is discontinuous at } u\}$.

Gimse and Risebro [9, 10] investigated a related problem corresponding to a piecewise constant velocity field in the equation $u_t + (V(x) f(u))_x = 0$. They constructed a weak solution, and proposed another condition, called minimum jump, to ensure uniqueness.

Next, we show that the construction above is well-defined. Let $u_1 < u_2 < \cdots < u_M$ be the values u can take. A curve of discontinuity of u is called a *shock front* or simply a front. A shock front where u has the value u_i on one side and u_j on the other side, is said to contain $|i - j|$ shock lines. The following result can be proved by slightly modifying the proof of Theorem 2.1 in Holden *et al.* [15]:

Lemma 2.2. *Let $\{\tau_i\}$ be all the points such that* $\operatorname{sgn} V(x, \tau_i^-) \neq \operatorname{sgn} V(x, \tau_i^+)$. *Let N be the number of intervals where f is linear. Let $L(t)$ be the number of shock lines in $u(\cdot, t)$ and $F(t)$ the number of shock fronts. Then the function*

$$G(t) = L(t)N + F(t)$$

is strictly decreasing for every shock collision in the intervals $t \in (\tau_i, \tau_{i+1})$.

The result means that the total number of shock fronts is bounded between each restart in the algorithm. If u_0 has a finite number of steps and if f is linear on a finite number of intervals, then $u(x,t)$ is constant on a finite number of domains. Suppose that $|V| < M$ and $|f'| < K$. Then the values of u_0 outside the interval $[x - MKt, x + MKt]$ do not influence

$u(x,t)$. So, even for an infinite number of steps in u_0, the construction is well-defined provided the number of restarts is finite.

The solution satisfies a maximum principle by construction, $\|u\|_\infty \le \|u_0\|_\infty$. Furthermore, all waves have finite speed of propagation and the L^1-norm is therefore Lipschitz continuous, $\|u(t_2) - u(t_1)\|_1 \le C|t_2 - t_1|$. Diminishing total variation is proved as follows: When two or more fronts collide, at least three values must meet. Let $u_1, \dots, u_K$ be the values that meet in the collision. After the collision, there will be at least one new shock front, unless the values u_1 and u_K are equal. When $u_1 = u_K$, all the intermediate values disappear and the total variation decreases in the collision. If the collision produces new shocks, u_1 will be the value to the left of the leftmost shock and u_K the value to the right of the rightmost shock, and the values in between will form a monotone sequence. Accordingly, all of the values $u_2, \dots, u_{K-1}$ that are not between u_1 and u_K disappear and the total variation decreases. At each restart in the algorithm the wave structure may change, but this does not increase the total variation.

The observations can be summarized in the following lemma:

Lemma 2.3. *Suppose that f is continuous and piecewise linear, V is as in Lemma 2.1, and u_0 is a bounded step function of bounded variation. Then the solution of $u_t + V(x,t)f(u)_x = 0$ satisfies*

$$\|u\|_\infty \le \|u_0\|_\infty, \quad \|u(t_2) - u(t_1)\|_1 \le C|t_2 - t_1|, \quad \mathrm{TV}(u) \le \mathrm{TV}(u_0). \tag{7}$$

In the case of general data for (1) we can approximate f by a piecewise linear function, u_0 by a piecewise constant function, and possibly V by a suitable function such that the assumptions in Lemma 2.1 are satisfied. This will give a family $\{u^\Delta(t)\}$ of approximate solutions. Now by using Lemma 2.3, a diagonalization process, and a standard application of Helly's theorem (see for instance Ref. [28]), we can show that there exists a convergent subsequence of $\{u^\Delta(t)\}$. Moreover, this sequence converges in $L^1_{\mathrm{loc}}(\mathbf{R} \times [0,T])$ for any $T > 0$, and the limit $u(x,t)$ is the solution of (1). The above construction is valid for all velocity fields that are Lipschitz continuous in x and possibly discontinuous in t, since each shock path then is the solution of a Caratheodory differential equation. Moreover, the velocity field may be discontinuous in x as long as the sign is preserved across each discontinuity.

Having constructed a weak solution to (1) by a limiting process, our next task is to prove that this solution is also an *entropy weak* solution. Kružkov [21] proved the existence of an entropy solution having a linear modulus (i.e., bounded variation) for the more general equation

$$u_t + \frac{d}{dx}\varphi(x,t,u) + \psi(x,t,u) = 0 \tag{8}$$

under certain assumptions on φ and ψ. He suggested an entropy condition to identify the unique physical solution: u is an entropy solution of (8), if for all constants k and all $\phi \in C^1_0$, the following inequality is valid

$$\begin{aligned} 0 \le \iint_{\mathcal{D}_T} \big\{ &|u-k|\phi_t + \mathrm{sgn}(u-k)[\varphi(x,t,u) - \varphi(x,t,k)]\phi_x \\ &- \mathrm{sgn}(u-k)[\varphi_x(x,t,k) - \psi(x,t,u)]\phi \big\}\, dxdt \\ &+ \int_{\mathbf{R}} |u(x,0) - k|\phi(x,0)\, dx \;-\; \int_{\mathbf{R}} |u(x,T) - k|\phi(x,T)\, dx. \end{aligned}$$

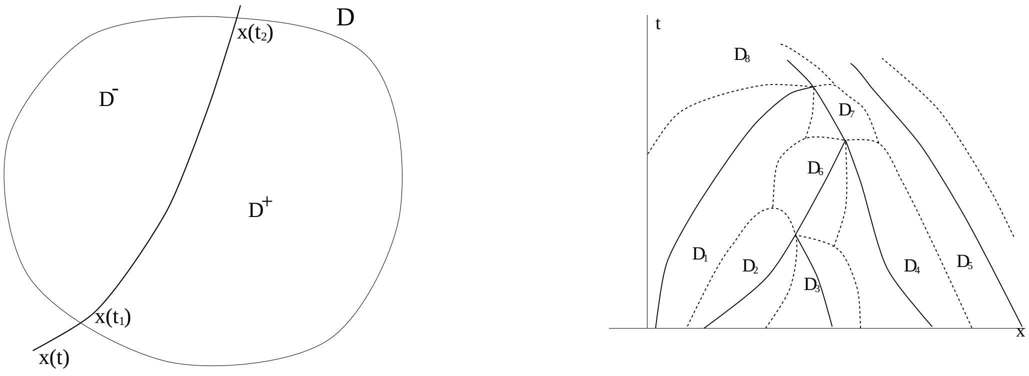

FIGURE 1. (Left) Domain for integration around a shock curve. (Right) The global domain divided into subdomains. The solid lines are shock curves and the dotted lines boundaries between subdomains.

This condition both defines a generalised (or weak) solution, and characterises permissible discontinuities.

We can now prove that both the approximate solutions and the limit satisfy a Kružkov entropy condition. To do so, we once more assume that V is differentiable with respect to x. By construction, an approximate solution is constant within the subdomain bounded by the shock paths (and the lines $t = 0$ and $t = \tau_i$). Choose a domain D such that it contains only one shock curve $x(t)$, see Figure 1. The solution is constant (and therefore smooth) in D, except along the curve $x(t)$. Assume that the solution attains the values u^+ and u^- in D^+ and D^-, respectively. Let ϕ be a test function with compact support in D. By construction, the solution then satisfies equation (2). The same is true for any constant k. Choosing $k > \sup u(x,t)$, gives $\operatorname{sgn}(u-k) = -1$ and $|u-k| = k-u$. The (in)equality is then derived by subtracting (2) with u from (2) with k

$$0 = \iint\limits_D \left\{ |u-k|\phi_t + \operatorname{sgn}(u-k)[f(u)-f(k)]\big(V(x,t)\phi\big)_x \right\} dtdx.$$

A similar argument is valid for $k < \inf u(x,t)$, and it remains to establish the inequality for $k \in [\inf u(x,t), \sup u(x,t)]$. We substitute $u = k$ in (3), multiply by $|V(x,t)|$, and use the Rankine-Hugoniot condition (4). The entropy condition now reads

$$V(x,t)\frac{f(u^+)-f(k)}{u^+-k} \leq \frac{dx}{dt} \leq V(x,t)\frac{f(u^-)-f(k)}{u^--k}$$

for any constant k between u^+ and u^-. This inequality may be further rearranged to

$$\begin{aligned}-|u^+-k|\frac{dx}{dt} &+ \operatorname{sgn}(u^+-k)[f(u^+)-f(k)]V(x,t) \\ &\leq -|u^--k|\frac{dx}{dt} + \operatorname{sgn}(u^--k)[f(u^-)-f(k)]V(x,t).\end{aligned}$$

We multiply by a test function, integrate the inequality along $x(t)$ from t_1 to t_2, and use the divergence theorem to derive the desired inequality on the domain D

$$\begin{aligned}0 &\le \int_{\partial D^-} \operatorname{sgn}(u^- - k)\phi(x,t)\big\langle u^- - k, [f(u^-) - f(k)]V(x(t),t)\big\rangle \cdot \vec{n}_{\partial D^-}\, ds \\ &\quad + \int_{\partial D^+} \operatorname{sgn}(u^+ - k)\phi(x,t)\big\langle u^+ - k, [f(u^+) - f(k)]V(x(t),t)\big\rangle \cdot \vec{n}_{\partial D^+}\, ds \\ &= \iint\limits_D \big\{|u-k|\phi_t + \operatorname{sgn}(u-k)[f(u)-f(k)]\big(V(x,t)\phi\big)_x\big\}\, dxdt.\end{aligned}$$

The next step is to divide the global domain into a countable number of subdomains D_i, as in Figure 1, and use the above inequality for each subdomain. Note that the compact support of ϕ in D_i was superfluous, since contributions along the boundaries of subdomains cancel when added together. The only exceptions are along the lines $t = 0$ and $t = T$. Hence, we have verified that the constructed solution satisfies the Kružkov condition

$$\begin{aligned}0 \le &\iint\limits_{\mathcal{D}_T} \big\{|u-k|\phi_t + \operatorname{sgn}(u-k)[f(u)-f(k)]\big(V(x,t)\phi\big)_x\big\}\, dtdx \\ &+ \int_{\mathbf{R}} |u(x,0) - k|\phi(x,0)\, dx - \int_{\mathbf{R}} |u(x,T) - k|\phi(x,T)\, dx.\end{aligned} \tag{9}$$

By using the bounded convergence theorem for Lebesgue integrals, the same result follows for general data, provided V is Lipschitz continuous in x. This gives an alternative proof for the existence of a solution of (1) satisfying the entropy condition (9).

3. Continuous Dependence

We now investigate how the variable coefficient equation (1) is sensitive to changes in flux function, velocity field, and initial data. In other words, we determine the difference in L^1–norm for solutions of the two equations

$$u_t + U(x,t)f(u)_x = 0, \qquad u(x,0) = u_0(x), \tag{10}$$

$$v_t + V(x,t)g(v)_x = 0, \qquad v(x,0) = v_0(x). \tag{11}$$

The method of analysis goes back to the seminal papers of Kružkov [21] and Kuznetsov [22] and has a strong flavour of the approach taken in [34].

The entropy conditions corresponding to (10), (11) are on the form (9). Here v_0, V, and g are considered as perturbations of u_0, U, and f. Assume that U and V are continuous and possess derivatives U_x and V_x. Let $\mathcal{D}_T$ denote the domain $\mathbf{R} \times [0,T]$. Once we have establish continuous dependence, an error bound follows immediately as we will see in Section 4.

Let us first construct a suitable class of test functions. Assume that $\omega \in C_0^\infty(\mathbf{R})$ is a non-negative, even function such that $\int_{\mathbf{R}} \omega(x)dx = 1$, $\operatorname{sgn}(x)\omega'(x) \le 0$, and $\omega(x) \equiv 0$ for $|x| \ge 1$. Then $\int_{\mathbf{R}} |x|\,|\omega'(x)|dx = 1$. For any $\varepsilon > 0$ define the function $\omega_\varepsilon(x) = \varepsilon^{-1}\omega(x/\varepsilon)$. Then there is a constant M_ω, independent of ε, such that $|\omega_\varepsilon(x)| \le M_\omega/\varepsilon$ and $|\omega'_\varepsilon(x)| \le M_\omega/\varepsilon^2$ for all x. Based on ω_ε, we construct test functions

$$\phi^\varepsilon = \phi^\varepsilon(x-y, t-\tau) = \omega_\varepsilon(x-y)\,\omega_\varepsilon(t-\tau).$$

For later use, introduce the following shorthand notations

$$F(w,z) = \operatorname{sgn}(w-z)[f(w)-f(z)],$$
$$\Gamma_\varepsilon(w,z) = \iint_{\mathbf{R}^2} |w(x)-z(y)|\omega_\varepsilon(x-y)\,dxdy.$$

Choose test function ϕ^ε and constant $v(y,\tau)$ in the entropy condition for (10). After integration with respect to τ and y, it reads

$$0 \le \iint_{\mathcal{D}_T}\iint_{\mathcal{D}_T} \left\{|u(x,t)-v(y,\tau)|\phi_t^\varepsilon + F(u(x,t),v(y,\tau))\big(U(x,t)\phi^\varepsilon\big)_x\right\} dtdxd\tau dy$$
$$+\int_0^T \Gamma_\varepsilon(u(\cdot,0),v(\cdot,\tau))\omega_\varepsilon(\tau)\,d\tau - \int_0^T \Gamma_\varepsilon(u(\cdot,T),v(\cdot,\tau))\omega_\varepsilon(T-\tau)\,d\tau.$$

Similarly, let the entropy condition for (11) be given in the variables (y,τ), choose $k=u(x,t)$, and integrate with respect to x and t to get a similar inequality. Note that $\phi_x^\varepsilon = -\phi_y^\varepsilon$ and $\phi_t^\varepsilon = -\phi_\tau^\varepsilon$. Taking this and the symmetry of ϕ^ε into account, we add the two integrated entropy conditions to obtain

$$\int_0^T \Gamma_\varepsilon(u(\cdot,T),v(\cdot,\tau))\omega_\varepsilon(T-\tau)\,d\tau + \int_0^T \Gamma_\varepsilon(v(\cdot,T),u(\cdot,t))\omega_\varepsilon(T-t)\,dt$$
$$\le \int_0^T \Gamma_\varepsilon(u(\cdot,0),v(\cdot,\tau))\omega_\varepsilon(0-\tau)\,d\tau + \int_0^T \Gamma_\varepsilon(v(\cdot,0),u(\cdot,t))\omega_\varepsilon(0-t)\,dt$$
$$+\iint_{\mathcal{D}_T}\iint_{\mathcal{D}_T} \phi_x^\varepsilon\left[F(u(x,t),v(y,\tau))U(x,t) - G(u(x,t),v(y,\tau))V(y,\tau)\right] dtdxd\tau dy$$
$$+\iint_{\mathcal{D}_T}\iint_{\mathcal{D}_T} \phi^\varepsilon\left[F(u(x,t),v(y,\tau))U_x(x,t) + G(u(x,t),v(y,\tau))V_y(y,\tau)\right] dtdxd\tau dy.$$

The inequality above may be written as

$$L_1(\varepsilon) + L_2(\varepsilon) \le R_1(\varepsilon) + R_2(\varepsilon) + R_3(\varepsilon) + R_4(\varepsilon). \tag{12}$$

The dependence result will follow by bounding the terms as ε tends to zero.

Starting with the left-hand side, we can show that

$$\lim_{\varepsilon\to 0} L_1(\varepsilon) = \frac{1}{2}\int_{\mathbf{R}} |u(x,T)-v(x,T)|\,dx.$$

Since the test function ω_ε has compact support for $|x|\le\varepsilon$ and integrates to unity, it follows that $\int_0^T \omega_\varepsilon(T-t)\,dt = 1/2$. Therefore

$$\left|L_1(\varepsilon) - \frac{1}{2}\int_{\mathbf{R}} |u(x,T)-v(x,T)|\,dx\right|$$
$$\le \frac{M_\omega}{\varepsilon}\int_{\mathbf{R}}\int_{T-\varepsilon}^T |v(y,\tau)-v(y,T)|\,dyd\tau + \frac{1}{2}\frac{M_\omega}{\varepsilon}\int_{\mathbf{R}}\int_{x-\varepsilon}^{x+\varepsilon} |v(x,T)-v(y,T)|\,dydx.$$

Using a lemma proved by Kružkov [21, Lemma 2] we see that both terms on the right-hand side of the inequality tend to zero with ε. A similar argument may be used to prove that

$$\begin{aligned}\lim_{\varepsilon\to 0}\big[L_1(\varepsilon)+L_2(\varepsilon)\big] &= \int_{\mathbf{R}}|u(x,T)-v(x,T)|\,dx = \|u(\cdot,T)-v(\cdot,T)\|_1,\\ \lim_{\varepsilon\to 0}\big[R_1(\varepsilon)+R_2(\varepsilon)\big] &= \int_{\mathbf{R}}|u(x,0)-v(x,0)|\,dx = \|u_0-v_0\|_1.\end{aligned}$$

For $R_4(\varepsilon)$ we observe that

$$\begin{aligned}|R_4(\varepsilon)| \le &\iint\limits_{\mathcal{D}_T}\iint\limits_{\mathcal{D}_T}\phi^\varepsilon|f(u(x,t))-f(v(y,\tau))||U_x(x,t)|\,dtdxd\tau dy\\ &+\iint\limits_{\mathcal{D}_T}\iint\limits_{\mathcal{D}_T}\phi^\varepsilon|g(u(x,t))-g(v(y,\tau))||V_y(y,\tau)|\,dtdxd\tau dy\\ \le&\big(\|f\|_{\mathrm{Lip}}\|U_x\|_\infty+\|g\|_{\mathrm{Lip}}\|V_x\|_\infty\big)\iint\limits_{\mathcal{D}_T}\iint\limits_{\mathcal{D}_T}\phi^\varepsilon|u(x,t)-v(y,\tau)|\,dtdxd\tau dy\end{aligned}$$

and repeat the argument used for $L_1(\varepsilon)$ to yield the upper bound

$$\lim_{\varepsilon\to 0}|R_4(\varepsilon)| \le \big(\|f\|_{\mathrm{Lip}}\|U_x\|_\infty+\|g\|_{\mathrm{Lip}}\|V_x\|_\infty\big)\int_0^T\|u(\cdot,t)-v(\cdot,t)\|_1\,dt.$$

The remaining term $R_3(\varepsilon)$ must be split into two terms $R_{31}(\varepsilon)+R_{32}(\varepsilon)$, one with a difference in velocity fields and one with a difference in flux functions. There are two possible ways of rearranging the integrand

$$FU-GV = F(U-V)+(F-G)V = G(U-V)+(F-G)U.$$

Here we choose the first form. Because the two velocity fields U and V in $R_{31}(\varepsilon)$ are evaluated at different variables (x,t) and (y,τ), this term must be further rearranged. Since ω_ε has compact support, $\int_{\mathbf{R}}h(y)\omega_\varepsilon'(x)dx = 0$ for any integrable function h. Thus $R_{31}(\varepsilon)$ may be rewritten as follows

$$\begin{aligned}R_{31}(\varepsilon) &= \iint\limits_{\mathcal{D}_T}\iint\limits_{\mathcal{D}_T}F(u(x,t),v(y,\tau))[U(x,t)-V(y,\tau)]\phi^\varepsilon_x(x-y,t-\tau)\,dtdxd\tau dy\\ &= \iint\limits_{\mathcal{D}_T}\iint\limits_{\mathcal{D}_T}\big[F(u(x,t),v(y,\tau))[U(x,t)-V(y,\tau)]\\ &\qquad\qquad -F(u(y,t),v(y,\tau))[U(y,t)-V(y,\tau)]\big]\phi^\varepsilon_x(x-y,t-\tau)\,dtdxd\tau dy.\end{aligned}$$

The integrand (except the test function) can be manipulated to yield three terms

$$\begin{aligned}F(x,t,y,\tau)&[U(x,t)-V(y,\tau)]-F(y,t,y,\tau)[U(y,\tau)-V(y,\tau)]\\ &=F(x,t,y,\tau)[U(x,t)-U(y,t)]\\ &\quad+[F(x,t,y,\tau)-F(y,t,y,\tau)][(U(y,t)-U(y,\tau))+(U(y,\tau)-V(y,\tau))],\end{aligned}$$

and the integral is split in three parts

$$R_{31}(\varepsilon) = R_{311}(\varepsilon)+R_{312}(\varepsilon)+R_{313}(\varepsilon).$$

Using the symmetry, the integrand of $R_{31}(\varepsilon)$ could have been rearranged using V instead of U. The first term $R_{311}(\varepsilon)$ is straightforward to dominate

$$
\begin{aligned}
|R_{311}(\varepsilon)| &\leq \iint\limits_{\mathcal{D}_T} \iint\limits_{\mathcal{D}_T} |F(u(x,t), v(y,\tau))|\, |U(x,t) - U(y,t)|\, |\phi_x^\varepsilon(x-y, t-\tau)|\, dt dx d\tau dy \\
&\leq \|U_x\|_\infty \|f\|_{\mathrm{Lip}} \iint\limits_{\mathcal{D}_T} \iint\limits_{\mathcal{D}_T} |u(x,t) - v(y,\tau)|\, |x-y|\, |\phi_x^\varepsilon(x-y, t-\tau)|\, dt dx d\tau dy.
\end{aligned}
$$

Recall that $\int_{\mathbf{R}} |x||\omega_\varepsilon'(x)|dx = 1$ and that $\phi_y^\varepsilon = -\phi_x^\varepsilon$. Thus

$$
\int\limits_{\mathbf{R}} |u(x,t) - v(x,t)| dx = \int\limits_{\mathbf{R}} \iint\limits_{\mathcal{D}_T} |u(x,t) - v(x,t)|\, |x-y|\, |\phi_x^\varepsilon(x-y, t-\tau)|\, dx d\tau dy.
$$

Since $|x-y|\, |\phi_x^\varepsilon(x-y, t-\tau)| \leq M_\omega/\varepsilon$, we can repeat the argument for $L_1(\varepsilon)$ and obtain

$$
\lim_{\varepsilon \to 0} |R_{311}(\varepsilon)| \leq \|U_x\|_\infty \|f\|_{\mathrm{Lip}} \int_0^T \|u(\cdot,t) - v(\cdot,t)\|_1\, dt.
$$

If the function $f(u)$ satisfies a Lipschitz condition on the interval $[-M, M]$ with constant L, then the function $F(u,v) = \mathrm{sgn}(u-v)[f(u) - f(v)]$ also satisfies the Lipschitz condition in u and v with the constant L, see [21, Lemma 3]. Hence it follows that

$$
\begin{aligned}
|R_{312}(\varepsilon)| &\leq \iint\limits_{\mathcal{D}_T} \iint\limits_{\mathcal{D}_T} |U(y,t) - U(y,\tau)|\, |F(u(x,t), v(y,\tau)) - F(u(y,t), v(y,\tau))|\, |\phi_x^\varepsilon|\, dt dx d\tau dy \\
&\leq \sup_{\tau, t < T, |t-\tau| < \varepsilon} \|U(\cdot,t) - U(\cdot,\tau)\|_\infty \|f\|_{\mathrm{Lip}} \iint\limits_{\mathcal{D}_T} \iint\limits_{\mathcal{D}_T} |u(x,t) - u(y,t)|\, |\phi_x^\varepsilon|\, dt dx d\tau dy
\end{aligned}
$$

since $\omega_\varepsilon(t-\tau)$ is zero when $|t-\tau| \geq \varepsilon$. For the integral $I(\varepsilon)$, we use that $\omega_\varepsilon(x)$ and $|x|\, |\omega_\varepsilon'(x)|$ integrate to unity and find that

$$
\begin{aligned}
I(\varepsilon) &\leq \int\limits_{\mathbf{R}} \iint\limits_{\mathcal{D}_T} |u(x,t) - u(y,t)|\, |\omega_\varepsilon(x-y)_x|\, dx dy dt \\
&= \iint\limits_{\mathcal{D}_T} |\omega_\varepsilon'(z)|\, |z| \int\limits_{\mathbf{R}} \frac{|u(x,t) - u(x-z,t)|}{|z|}\, dx dz dt \ \leq\ T\, \mathrm{TV}(u_0).
\end{aligned}
$$

Now introduce the shorthand $\nu_T(U) = \sup_{0<t<T} |\|U(\cdot,t^+) - U(\cdot,t^-)\|_\infty$. Thus we have

$$
\lim_{\varepsilon \to 0} |R_{312}(\varepsilon)| \leq \nu_T(U) \|f\|_{\mathrm{Lip}} T\, \mathrm{TV}(u_0).
$$

Note that if $U(\cdot,t)$ is continuous, $R_{312}(\varepsilon) \to 0$.

We have now established the dependence on initial data. Suppose that $u(x,t)$ and $v(x,t)$ are two solutions of (1), with initial data u_0 and v_0. Let $\{\tau_i\}$ denote the discontinuities in the velocity field, that is, $U(x,\tau_i^-) \neq U(x,\tau_i^+)$ for $i > 0$, and let $\tau_0 = 0$. Then for $t \in [\tau_i, \tau_{i+1}\rangle$

$$
\|u(\cdot,t) - v(\cdot,t)\|_1 \leq \|u(\cdot,\tau_i^+) - v_{(}\cdot,\tau_i^+)\|_1 + \gamma \int_{\tau_i^+}^t \|u(\cdot,s) - v(\cdot,s)\|_1\, ds
$$

for a finite constant $\gamma = 3\|V_x\|_\infty \|f\|_{\mathrm{Lip}}$. Applying a Gronwall inequality gives

$$\|u(\cdot,t) - v(\cdot,t)\|_1 \le e^{\gamma(t-\tau_i^+)} \|u(\cdot,\tau_i^+) - v(\cdot,\tau_i^+)\|_1.$$

This inequality can be used to prove uniqueness of the solution. Obviously

$$\|u(\cdot,\tau_i^+) - u(\cdot,\tau_i^-)\|_1 = 0,$$

and by choosing equal initial data $u_0 = v_0$, the uniqueness follows by induction on i.

To establish the continuous dependence on flux function and velocity field, the two remaining terms $R_{313}(\varepsilon)$ and $R_{32}(\varepsilon)$ need to be bounded. Fortunately, most of the work has already been done

$$\begin{aligned}
|R_{313}(\varepsilon)| \le& \iint\limits_{\mathcal{D}_T} \iint\limits_{\mathcal{D}_T} |U(y,t) - V(y,\tau)| \, |F(u(x,t),v(y,\tau)) - F(u(y,t),v(y,\tau))| \, |\phi_x^\varepsilon| \, dt dx d\tau dy \\
\le& \|U - V\|_\infty \|f\|_{\mathrm{Lip}} \iint\limits_{\mathcal{D}_T} \iint\limits_{\mathcal{D}_T} |u(x,t) - u(y,t)| \, |\omega_\varepsilon(x-y)_x| \, \omega_\varepsilon(t-\tau) \, dt dx d\tau dy \\
\to& T\|U - V\|_\infty \|f\|_{\mathrm{Lip}} \, \mathrm{TV}(u_0).
\end{aligned}$$

Using once more that $\int_{\mathbf{R}} h(y)\omega_\varepsilon'(x)dx = 0$, it follows that

$$\begin{aligned}
R_{32}(\varepsilon) =& \iint\limits_{\mathcal{D}_T} \iint\limits_{\mathcal{D}_T} (G - F)(u(x,t),v(y,\tau)) V(y,\tau) \phi_x^\varepsilon(x-y,t-\tau) \, dt dx d\tau dy \\
=& \iint\limits_{\mathcal{D}_T} \iint\limits_{\mathcal{D}_T} \phi_x^\varepsilon \big\{ (G-F)(u(x,t),v(y,\tau)) - (G-F)(u(y,t),v(y,\tau)) \big\} V(y,\tau) \, dt dx d\tau dy \\
\le& \|f - g\|_{\mathrm{Lip}} \|V\|_\infty \iint\limits_{\mathcal{D}_T} \iint\limits_{\mathcal{D}_T} |u(x,t) - u(y,t)| \, |\omega_\varepsilon(x-y)_x| \omega_\varepsilon(t-\tau) \, dt dx d\tau dy \\
\to& T\|f - g\|_{\mathrm{Lip}} \|V\|_\infty \, \mathrm{TV}(u_0).
\end{aligned}$$

All bounds can be summarized in the inequality

$$\|u(\cdot,T) - v(\cdot,T)\|_1 \le \|u_0 - v_0\|_1 + \gamma \int_0^T \|u(\cdot,t) - v(\cdot,t)\|_1 \, dt + \lambda T \, \mathrm{TV}(u_0),$$

where

$$\begin{aligned}
\gamma =& 2\|U_x\|_\infty \|f\|_{\mathrm{Lip}} + \|V_x\|_\infty \|g\|_{\mathrm{Lip}}, \\
\lambda =& \|f\|_{\mathrm{Lip}} \big(\|U - V\|_\infty + \nu_T(U) \big) + \|V\|_\infty \|f - g\|_{\mathrm{Lip}}.
\end{aligned}$$

As pointed out above, there are two ways of rearranging $R_3(\varepsilon)$, and then two ways of rearranging $R_{31}(\varepsilon)$. Altogether, this gives four combinations, of which we have computed one explicitly here. The other three give similar estimates. To get a sharper bound, one should therefore choose the minimum of the four.

Either way, the inequality is on the form $E(T) \le E(0) + \gamma \int_0^T E(t)dt + B$. Applying a Gronwall type inequality gives $E(T) \le e^{\gamma T}(E(0) + B)$, and we arrive at our final result concerning the continuous dependence

Theorem 3.1. *Let u and v denote two entropy solutions of* (10) *and* (11)*, respectively. Suppose that U_x and V_x are bounded, and that f and g satisfy a Lipschitz condition. Then there are constants γ and λ such that*

$$\|u(\cdot,T)-v(\cdot,T)\|_1 \leq e^{\gamma T}\|u_0-v_0\|_1+\lambda T e^{\gamma T}\min\{\mathrm{TV}(u_0),\mathrm{TV}(v_0)\},$$

for every finite T.

The above result can be extended to velocity fields that are only Lipschitz continuous in x by using a smooth approximation. When $V(x,t)=U(x,t)\equiv 1$, γ is zero and λ is equal to $\|f-g\|_{\mathrm{Lip}}$, and the above inequality is simplified to that of Lucier [27, Theorem 3]. Moreover, by a tedious computation, the above stability result can be extended to multi-dimensional equations of the form

$$u_t+\sum_{i=1}^{d} V_i(x,t) f_i(u)_{x_i}=0, \qquad u(x,0)=u_0(x). \tag{13}$$

The multi-dimensional counterpart of the above bound is,

$$\|u(\cdot,T)-v(\cdot,T)\|_1 \leq \|u_0-v_0\|_1+\gamma\int_0^T \|u(\cdot,t)-v(\cdot,t)\|_1\,dt+\lambda C(T)\,\mathrm{TV}(u_0),$$

where

$$\gamma=\sum_{i=1}^{d} 2\|\partial_{x_i}U_i\|_\infty\|f_i\|_{\mathrm{Lip}}+\|\partial_{x_i}V_i\|_\infty\|g_i\|_{\mathrm{Lip}},$$

$$\lambda=\sum_{i=1}^{d}\|f_i\|_{\mathrm{Lip}}\big(\|U_i-V_i\|_\infty+\nu_T(U_i)\big)+\|V_i\|_\infty\|f_i-g_i\|_{\mathrm{Lip}}.$$

Note that these equations have bounded, but not necessarily diminishing total variation. Therefore the constant $T\,\mathrm{TV}(u_0)$ is replaced by $C(T)\,\mathrm{TV}(u_0)$.

4. A Front Tracking Method

In this section we look into how the front tracking construction from Section 2 can be utilized as a numerical method. The major difference between the current construction and Dafermos' method is the way the shock paths are given. In Dafermos' method the shock paths are given as straight lines, i.e., $x(t)=x_0+s(t-t_0)$, while in the current method they satisfy an ordinary differential equation $\dot{x}(t)=sV(x,t)$. Thus, to derive a fully discrete construction, we must be able to solve these ODEs, at least approximately. An important part of the front tracking is to determine possible wave interactions, i.e., compute intersections of two neighbouring shock paths.

Instead of introducing some numerical method for the ODEs, we will make piecewise polynomial approximations to the forcing velocity field so that the corresponding ODEs can be solved explicitly. For velocity fields that depend only on spatial position or time we propose to use a straightforward, piecewise linear approximation so that the shock paths are given by one of the formulas (5) or (6) on each interval in the approximation.

For velocities that depend on both x and t we use velocity approximations that are given by either $V(x,t)=(a_ix+b_i)c_j$ or $V(x,t)=a_i(c_jt+d_j)$ on the squares $[x_i,x_{i+1}]\times[t_j,t_{j+1})$. This simple form means that $\dot{x}(t)=sV(x,t)$ can be solved by separation of variables and combination of the expressions (5) and (6). The price we pay for this simplicity is loss of approximation order in either t or x.

As required in the front tracking construction, the grid cells in the above approximations (for time dependent velocity fields) are chosen such that $V(\cdot,t)$ has constant sign on each cell. Hence, the times $\{\tau_k\}$ where the algorithm is restarted (because V changes sign) forms a subset of $\{t_i\}$.

Although a piecewise constant approximation in x and t is not covered by the analysis in Section 3, it is possible from a constructive point of view and is in fact used in the commercial reservoir simulator *Frontline* [2].

When implementing the front tracking method, all shock fronts are represented as data objects in a linked list [31, 23] given by their spatial ordering from left to right. Similarly, all possible collisions are kept in a collision list. An obvious alternative is to use a priority queue in the form of a balanced binary tree. Here, however, we have chosen to implement the collision queue as a (doubly-linked) list. To establish the two lists we first solve all Riemann problems given by the initial approximation and then compute possible interactions. In the tracking part of the algorithm each step goes as follows: We find the next colliding fronts in the time list, remove them from the spatial list, and solve the corresponding Riemann problem. Possible new fronts are then inserted into the spatial list, and the collision list is updated. (Since we use a list for possible collisions, inserting a new front in the list is an $\mathcal{O}(n)$ operation, where n are the number of colliding fronts, and removing a front is an $\mathcal{O}(1)$ operation.)

To apply the same algorithm in our case, we need to settle two issues. First, how do we compute the path of fronts passing through several spatial intervals in the approximation of the velocity field? Somehow we must know when a front leaves a spatial interval and enters a new one. This is achieved by introducing dummy objects (i.e., artificial stationary 'fronts') in the spatial list to represent discontinuities in V or V_x. Thus, during the tracking of fronts there will be two kinds of front collisions: (i) between two shock fronts, and (ii) between a shock front and a discontinuity in V_x or V. For type (ii) collisions we simply exchange places for the colliding fronts in the spatial list and update the collision list. Introducing artificial fronts is also advantageous if we were to consider boundary value problems (especially for problems with moving boundaries).

The second problem is what to do when we reach a new temporal interval in the approximation of the velocity field. The obvious solution would be to simply restart the algorithm at each time $t = t_j$. However, we can be more clever. After each update in the time list we check if the next collision occurs in the current time interval $[t_j, t_{j+1})$. If not, we advance the solution forward in time to $t = t_{j+1}$ and compute the new velocity approximation. If the velocity field does not change sign anywhere, we need only reset the start positions of each front and update the collision list using the new velocity approximation. Notice that we do not need to solve any Riemann problems. However, if t_{j+1} coincides with a zero point τ_k in the velocity field, we have to restart the algorithm, by solving the Riemann problems described by the piecewise constant solution at time $t = t_{j+1}^-$.

In Section 2 we argued that there is a finite number of shock collisions if the number of initial jumps is finite. Assuming a finite number of intervals in the approximation of the velocity field, the number of updates to front paths remains finite. The efficiency of front tracking is retained if the additional work introduced by these extra collisions amounts little to the total work during the tracking. Obviously this is not the case if the length of the velocity intervals is small compared with the distance each shock travels before a collision. It is therefore important that intervals in the velocity approximation are fairly large, reducing the number of type (ii) shocks.

So, what about the convergence rate of the new front tracking method? Assume that $V = V(x)$ and let u denote the entropy solution of (1) and $\widetilde{u}$ the front tracking solution with flux function $\widetilde{f}$, velocity field $\widetilde{V}$, and initial data $\widetilde{u}_0$. Here Δ_f, Δ_V, and Δ_0 denote the length of the respective intervals. Then it follows from Theorem 3.1 that

$$\|u(\cdot,T) - \widetilde{u}(\cdot,T)\|_1 \leq C_1\|u_0 - \widetilde{u}_0\|_1 + C_2\|f - \widetilde{f}\|_{\mathrm{Lip}} + C_3\|V - \widetilde{V}\|_\infty,$$

where the constants C_1, C_2, and C_3 are finite and independent of the parameters Δ_f, Δ_V, and Δ_0. By a proper choice of the initial approximation, for instance the average function on each interval, we can ensure that $\|u_0 - \widetilde{u}_0\|_1 \leq C\Delta_0$. Assuming that f and V are Lipschitz continuous and piecewise C^2, we have that $\|f - \widetilde{f}\|_{\mathrm{Lip}} \leq \frac{1}{2}\Delta_f\|f''\|_\infty$ and $\|V - \widetilde{V}\|_\infty \leq C\Delta_V^2$. Thus, the error in the case of $V = V(x)$ is dominated in norm as follows

$$\|u(\cdot,T) - \widetilde{u}(\cdot,T)\|_1 \leq C_1\Delta_0 + C_2\Delta_f + C_3\Delta_V^2. \tag{14}$$

Hence, the convergence of the front tracking method remains linear when extended to the variable coefficient equation. It is also interesting to note that the convergence is quadratic in the approximation parameter for the velocity field if this field is only spatially dependent and possesses a certain regularity. This means that the velocity intervals may be chosen large to ensure an efficient algorithm. In the general case, however, we cannot ensure an $\mathcal{O}(\Delta_V^2)$ approximation by using piecewise linear approximations.

5. Numerical Experiments

Example 1. In the first example we study

$$u_t + V(x)f(u)_x = 0, \qquad u(x,0) = u_0(x)$$

with a nonconvex flux function $f(u) = 4u^2(1 - u^2)$ and non-monotone initial data $u_0(x)$ consisting of eight Riemann problems. The velocity field $V(x) = 0.75\sin(\pi x/2)$ changes sign at $x_n = 2n$, $n \in \mathbf{Z}$, and these points will therefore be stagnation points. Figure 2 shows the fronts in (x,t) space and the solution at four different times. The velocity field was approximated by a piecewise linear function on 90 equally spaced intervals. For the flux approximation we used 100 intervals.

Due to the symmetry of the initial data and the flux function and the *antisymmetry* of the velocity field, the solution is symmetric around $x = 0$ for all times. We therefore only discuss the dynamics for $x > 0$. The Riemann problem at $x = 0.5$ leads to two rarefaction waves separated by a stationary shock. The leftmost rarefaction wave propagates towards the stagnation point at the origin, giving fronts that asymptotically approach a vertical line in the (x,t) plane. Just before $t = 0.2$ the rightmost rarefaction wave interacts with the stationary shock from the Riemann problem at $x = 1.5$. This interaction produces a left-propagating shock followed by a rarefaction wave and a stationary shock (as seen in the (x,u) plot at time $t = 1.0$). At $t \approx 1.35$ the leftmost shock collides with the stationary shock at $x = 0.5$ to produce a centred rarefaction wave and a shock propagating towards the right (see (x,u) plot at time $t = 2.0$). At $t \approx 2.5$ this shock interacts with the stationary shock at $x = 1.5$ and produces a shock propagating towards the stagnation point at the origin, gradually eating up the rarefaction wave. The initial Riemann problem at $x = 3.0$ produces a centred rarefaction wave and a shock. The shock propagates towards the stagnation line at $x = 4.0$ and the shock

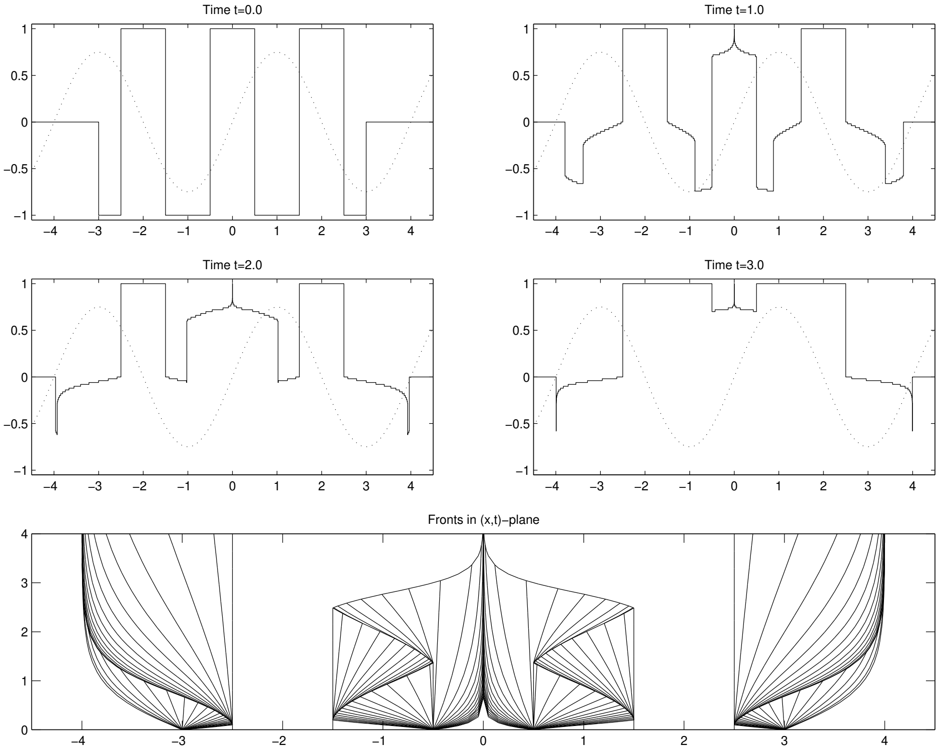

FIGURE 2. Example 1: solution in (x, u) and (x, t) plane. In the (x, u) plots, the velocity field is shown as a dotted line.

speed decays towards zero. At $t \approx 0.1$ the leftmost tail of the rarefaction wave reflects in the stationary shock at $x = 2.5$. The reflection produces a shock followed by a rarefaction wave (see (x, u) plot at $t = 1.0$). The shock speed decays towards zero as the shock approaches the stagnation point at $x = 4.0$.

Example 2. Next, we study Burgers' equation

$$u_t + V(x,t)\big(\tfrac{1}{2}u^2\big)_x = 0$$

with a time dependent velocity field $V(x, t) = \cos(\pi(x - t)/4)$ and piecewise constant initial data $u_0(x)$ equal unity on the interval $[-1/2, 1/2]$ and zero elsewhere over the spatial domain $[-1.0, 4.0]$.

Figure 3 shows snapshots of the solution computed up to time $t = 25.0$. The velocity approximation is piecewise linear in x on 10 equally spaced intervals and piecewise constant in t on 50 equally spaced intervals. The flux function is piecewise linear on 50 intervals between 0 and 1. The discretization parameters are chosen rather coarse to exemplify how the approximate solution is constructed.

The two initial Riemann problems give rise to a right-propagating shock wave followed by a rarefaction wave. The rarefaction wave overtakes the shock around $t = 2.75$. At the left end of the rarefaction wave, the fronts start to move backwards after time $t = 1.5$ due to negative velocity fields and eventually a shock is formed around $t = 3.25$. At time $t = 4.0$ the leading (rightmost) shock encounters negative values in the velocity field and is turned

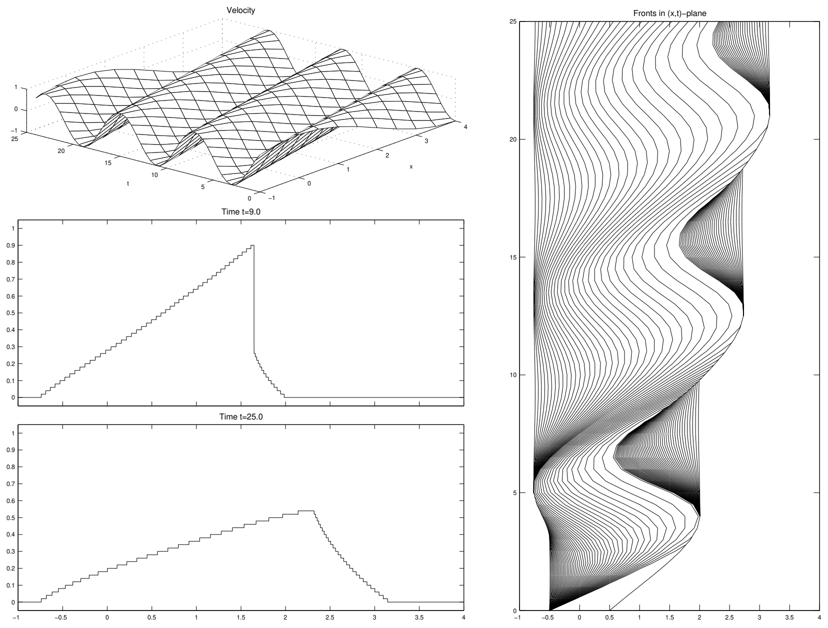

FIGURE 3. Example 2: solution and velocity field.

into a left-propagating rarefaction wave. The leftmost shock encounters positive values in the velocity field after $t = 5.0$ and becomes a right-propagating rarefaction wave. The right rarefaction wave turns at time $t = 6.5$, moves right again, and a shock is formed around $t = 8.0$. The shock is overtaken by the rarefaction wave, and so on.

Example 3. In the next example we seek to verify numerically the convergence rates derived in (14). To this end, we use Burgers' equation on the domain $[-2, 2]$ with velocity field $V(x) = \sin^3(\pi x/2)$ and initial data

$$u_0(x) = \begin{cases} 1, & x < -1, \\ -\sin^7(\pi x/2), & -1 \le x \le 1 \\ -1 & x > 1. \end{cases}$$

(The initial is a smoothed version of a step function with steps -1 to 0 and 0 to 1.) The solution at time $t = 1.0$ consists of three constant states $(-1, 0, 1)$ separated by a smooth wave and a shock. Numerical errors were measured relative to a reference solution generated with 2^{15} intervals in the initial approximation and 2^{13} intervals in the flux and velocity approximations. The convergence study was conducted as follows. We picked one parameter (say Δ_0) and refined it repeatedly by a factor two while keeping the other two parameters fixed at the reference level (i.e., $\Delta_f = 2^{-12}$ and $\Delta_V = 2^{-11}$). Table 1 shows the observed errors and the corresponding convergence rates. The results confirm the error estimate (14).

Example 4. In the last example we demonstrate how the front tracking method can be extended to systems and to multidimensions. To this end, we consider two-phase flow in a horizontal oil reservoir where oil is displaced either by water (secondary recovery) or by a mixture of water and polymer (tertiary recovery). The displacement process in both cases is

TABLE 1. *Example 3: observed errors and convergence rates for initial data (left), flux function (middle), and velocity field (right). Here n denotes the number of intervals in the approximation of each quantity.*

n	L^1-error	rate	n	L^1-error	rate	n	L^1-error	rate
32	1.576e-01	—	16	2.631e-02	—	32	1.978e-02	—
64	6.732e-02	1.23	32	1.316e-02	1.00	64	3.725e-03	2.41
128	3.240e-02	1.05	64	6.562e-03	1.00	128	1.016e-03	1.87
256	1.585e-02	1.03	128	3.267e-03	1.01	256	2.707e-04	1.91
512	7.794e-03	1.02	256	1.634e-03	1.00	512	6.525e-05	2.05
1024	3.819e-03	1.03	512	8.164e-04	1.00	1024	1.639e-05	1.99
2048	1.844e-03	1.05	1024	4.082e-04	1.00	2048	3.869e-06	2.08

described by a coupled system of nonlinear PDEs consisting of an elliptic equation for the pressure p

$$\nabla \cdot \big(k\lambda(u)\nabla p\big) = 0 \tag{15}$$

and a hyperbolic conservation law $u_t + V \cdot \nabla F(u) = 0$. The two equations are coupled through the Darcy velocity $V = -k\lambda(u)\nabla p$, where λ denotes the total mobility and k the reservoir permeability.

For tertiary recovery, the conservation law reads

$$\begin{bmatrix} s \\ sc + a(c) \end{bmatrix}_t + V \cdot \nabla \begin{bmatrix} f(s,c) \\ cf(s,c) \end{bmatrix} = 0, \tag{16}$$

where s denotes the water saturation, c the polymer concentration, and $a(c)$ is the adsorption function. The fractional flow function f has a typical S-shape. The model for the secondary recovery is a special case of (16) with $c \equiv 0$.

The system (15)–(16) is solved by a sequential operator splitting. First, the pressure equation (15) is solved with total mobility given by the initial distribution of water and polymer. Subsequently, the corresponding Darcy velocity is held fixed and the saturation/concentration is advanced forward a time step. The process is repeated until one reaches the desired time level, see e.g., [11] for more details.

To solve the multidimensional conservation law, we use dimensional splitting. That is, given u on a Cartesian mesh, we first solve $u_t + V_1\, F(u)_{x_1} = 0$ along each row in the mesh and then project the one-dimensional solutions onto the mesh again. Next, the same procedure is repeated for all columns in the mesh. For more details on this procedure, see [26].

The idea of using a piecewise linear approximation to the flux function does not apply in the case of a system. Instead, the method is reformulated as follows [30]: shocks and contact discontinuities are kept and rarefaction waves are approximated by step functions. This way, the Riemann solutions consist of constant states separated by space-time rays and the above construction applies. The front tracking method applied to the polymer system introduced above is described in [32].

We consider a quarter five-spot test case, consisting of a repeated pattern of squares with an injection well in the center and production wells at the corners $(\pm 1, \pm 1)$. Due to symmetry, we only simulate the first quadrant of the square. For the adsorption function and the fractional

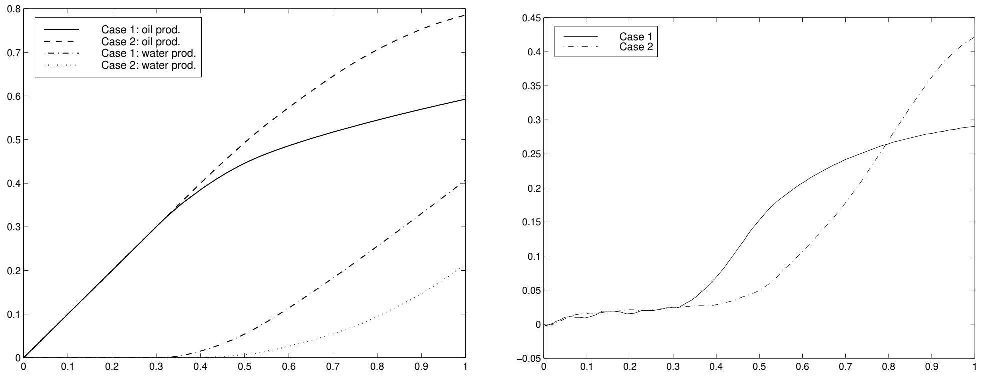

FIGURE 4. Example 4. (Left) Oil and water production for the two cases. (Right) Percentage mass balance error for water in the two cases.

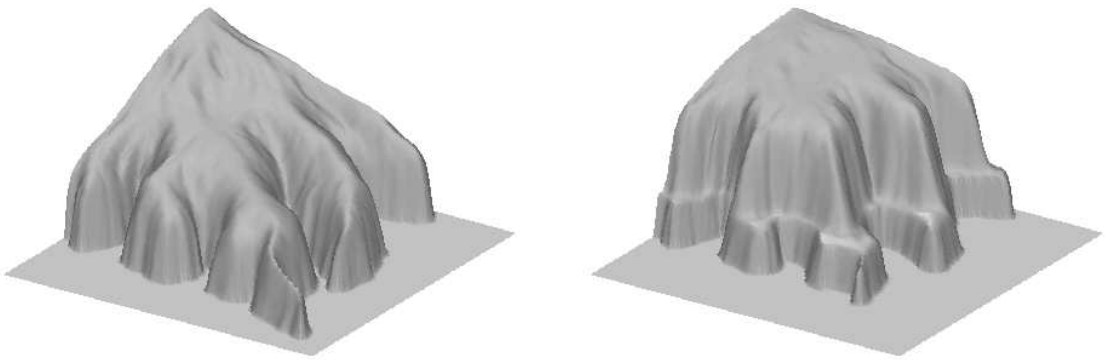

FIGURE 5. Example 4. Surface plot of the water saturation for Case 1 (left) and Case 2 (right).

flow function we use

$$a(c) = \frac{0.2c}{1+c}, \qquad f(s,c) = \frac{s^2}{s^2 + 0.2(1-s)^2(1+50c)}.$$

This corresponds to a viscosity ratio of 0.2 between water and oil. We consider two cases; in the first case, we inject pure water and in the second case we add polymer with a concentration 0.1. In both cases we use the same random permeability field.

Figure 4 shows a plot of the oil and water production for the two cases up to time $t = 1$ (corresponding to injection of one pore volume of water). In the first case, the injected water fingers through the oil because of the unfavourable viscosity ratio and gives an early water breakthrough (time $t = 0.314$) in the production well. By adding polymer to the injected fluid in the second case, we improve the mobility ration and obtain a later breakthrough (time $t = 0.387$). Moreover, the areal sweep of the injection well increases, which leads to a much higher oil production. Figure 5 shows surface plots of the water saturation at time $t = 0.3$ in both cases.

Due to dimensional splitting of the conservation law and approximation of rarefaction waves by step functions, the front tracking method is nonconservative. Figure 4 shows the mass balance error for the two simulations. Up to water breakthrough, the mass error is negligible, but increases as the water front approaches the singularity in the velocity field at the production well. However, the maximum error does not exceed 0.45%. Lack of mass conservation and grid orientation effects for simulation of the tertiary process is discussed thoroughly in [11]. Front tracking simulations for secondary recovery are found in [7, 16, 19, 26].

Acknowledgement

I would like to thank the late Sigmund Berntsen, Harald Hanche–Olsen, Vidar Haugse, Helge Holden, Kenneth Hvistendahl Karlsen, and Nils Henrik Risebro for many valuable discussions.

References

[1] L. M. Barker. Swap—a computer program for shock wave analysis. Technical Report No. SC4796(RR), Sandia Nat. Labs., Albuquerque, New Mexico, 1963.

[2] F. Bratvedt, K. Bratvedt, C. F. Buchholz, T. Gimse, H. Holden, L. Holden, and N. H. Risebro. FRONTLINE and FRONTSIM: two full scale, two-phase, black oil reservoir simulators based on front tracking. *Surveys Math. Indust.*, 3(3):185–215, 1993.

[3] A. Bressan, G. Crasta, and B. Piccoli. Well-posedness of the Cauchy problem for $n \times n$ systems of conservation laws. *Mem. Amer. Math. Soc.*, to appear.

[4] A. Bressan and P. LeFloch. Uniqueness of weak solutions to systems of conservation laws. *Arch. Rational Mech. Anal.*, 140(4):301–317, 1997.

[5] R. Bürger, S. Evje, K. Hvistendahl Karlsen, and K.-A. Lie. Numerical methods for the simulation of the settling of flocculated suspensions. Preprint 99/03, Sonderforschungsbereich 404, University of Stuttgart, Stuttgart, Germany.

[6] C. M. Dafermos. Polygonal approximation of solutions of the initial value problem for a conservation law. *J. Math. Anal. Appl.*, 38:33–41, 1972.

[7] S. Evje, K. H. Karlsen, K.-A. Lie, and N. H. Risebro. Front tracking and operator splitting for nonlinear degenerate convection–diffusion equations. In P. Bjørstad and M. Luskin, editors, *Parallel solution of partial differential equations*, IMA Vol. Math. Appl., Vol. 120, Springer, New York, 2000.

[8] T. Gimse. Conservation laws with discontinuous flux function. *SIAM J. Math. Anal.*, 24(2):279–289, 1993.

[9] T. Gimse and N. H. Risebro. Riemann problems with a discontinuous flux function. In *Proc. 3rd Internat. Conf. Hyperbolic Problems*, pages 488–502, Uppsala, 1991.

[10] T. Gimse and N. H. Risebro. Solution of the Cauchy problem for a conservation law with a discontinuous flux function. *SIAM J. Math. Anal.*, 23(3):635–648, 1992.

[11] V. Haugse, K. H. Karlsen, K.-A. Lie, and J. R. Natvig. Numerical solution of the polymer system by front tracking. Preprint, Department of Mathematics, University of Bergen, 1999.

[12] G. W. Hedstrom. Some numerical experiments with Dafermos's method for nonlinear hyperbolic equations. In *Numerische Lösung nichtlinearer partieller Differential- und Integrodifferentialgleichungen (Tagung, Math. Forschungsinst., Oberwolfach, 1971)*, pages 117–138. Lecture Notes in Math., Vol. 267. Springer, Berlin, 1972.

[13] G. W. Hedstrom. The accuracy of Dafermos' method for nonlinear hyperbolic equations. In *Proceedings of Equadiff III (Third Czechoslovak Conf. Differential Equations and their Applications, Brno, 1972)*, pages 175–178. Folia Fac. Sci. Natur. Univ. Purkynianae Brunensis, Ser. Monograph., Tomus 1. Purkyně Univ., Brno, 1973.

[14] H. Holden and L. Holden. On scalar conservation laws in one-dimension. In S. Albeverio, J. E. Fenstad, H. Holden, and T. Lindstrøm, editors, *Ideas and Methods in Mathematics and Physics*, pages 480–509. Cambridge University Press, Cambridge, 1988.

[15] H. Holden, L. Holden, and R. Høegh-Krohn. A numerical method for first order nonlinear scalar conservation laws in one-dimension. *Comput. Math. Applic.*, 15(6–8):595–602, 1988.

[16] H. Holden, K. H. Karlsen, and K.-A. Lie. Operator splitting methods for degenerate convection–diffusion equations II: Numerical examples with emphasis on reservoir simulation. Preprint, 1999.

[17] L. Holden. The Buckley-Leverett equation with spatially stochastic flux function. *SIAM J. Appl. Math.*, 57(5):1443–1454, 1997.

[18] K. H. Karlsen and K.-A. Lie. An unconditionally stable splitting for a class of nonlinear parabolic equations. *IMA J. Numer. Anal.*, 19(4):609–635, 1999.

[19] K. H. Karlsen, K.-A. Lie, N. H. Risebro, and J. Frøyen. A front-tracking approach to a two-phase fluid-flow model with capillary forces. *In Situ*, 22(1):59–89, 1998.
[20] C. Klingenberg and N. H. Risebro. Convex conservation laws with discontinuous coefficients. Existence, uniqueness and asymptotic behavior. *Comm. Partial Differential Equations*, 20(11-12):1959–1990, 1995.
[21] S. N. Kružkov. First order quasi-linear equations in several independent variables. *Math. USSR Sbornik*, 10(2):217–243, 1970.
[22] N. N. Kuznetsov. Accuracy of some approximative methods for computing the weak solutions of a first-order quasi-linear equation. *USSR Comput. Math. and Math. Phys. Dokl.*, 16(6):105–119, 1976.
[23] J. O. Langseth. On an implementation of a front tracking method for hyperbolic conservation laws. *Advances in Engineering Software*, 26(1):45–63, 1996.
[24] R. J. LeVeque. Large time step shock-capturing techniques for scalar conservation laws. *SIAM J. Numer. Anal.*, 19(6):1091–1109, 1982.
[25] R. J. LeVeque. A large time step generalization of Godunov's method for systems of conservation laws. *SIAM J. Numer. Anal.*, 22(6):1051–1073, 1985.
[26] K.-A. Lie. A dimensional splitting method for nonlinear equations with variable coefficients. *BIT*, 39(4):683–700, 1999.
[27] B. J. Lucier. A moving mesh numerical method for hyperbolic conservation laws. *Math. Comp.*, 46(173):59–69, 1986.
[28] O. A. Oleinik. Discontinuous solutions of non-linear differential equations. *Amer. Math. Soc Transl. Ser. 2*, 26:95–172, 1963.
[29] O. A. Oleinik. Uniqueness and stability of the generalized solution of the Cauchy problem for a quasi–linear equation. *Amer. Math. Soc Transl. Ser. 2*, 33:285–290, 1963.
[30] N. H. Risebro. A front-tracking alternative to the random choice method. *Proc. Amer. Math. Soc.*, 117(4):1125–1139, 1993.
[31] N. H. Risebro and A. Tveito. A front tracking method for conservation laws in one dimension. *J. Comp. Phys.*, 101(1):130–139, 1992.
[32] N. H. Risebro and A. Tveito. Front tracking applied to a nonstrictly hyperbolic system of conservation laws. *SIAM J. Sci. Stat. Comput.*, 12(6):1401–1419, 1991.
[33] B. K. Swartz and B. Wendroff. AZTEC: a front tracking code based on Godunov's method. *Appl. Numer. Math.*, 2(3-5):385–397, 1986.
[34] A. Tveito and R. Winther. Existence, uniqueness, and continuous dependence for a system of hyperbolic equations modeling polymer flooding. *SIAM J. Math. Anal.*, 22(4):905–933, 1991.
[35] Y. S. Zheng. A note on Dafermos' polygonal approximation method. *J. Math. Res. Exposition*, 4(1):65–66, 1984. (In Chinese).

SINTEF Applied Mathematics, P.O. Box 124 Blindern, N–0314 Oslo, Norway
E-mail address: `Knut-Andreas.Lie@math.sintef.no`

Department of Informatics, University of Oslo, P.O. Box 1080 Blindern, N–0316 Oslo
E-mail address: `kalie@ifi.uio.no`
URL: `http://www.ifi.uio.no/~kalie/`